International Journal of Engineering Sciences Paradigms and Researches (IJESPR)
(Vol. 39, Issue 01) and (Publishing Date: 21st February, 2017)
(An Indexed, Referred and Impact Factor Journal)
ISSN: 2319-6564
www.ijesonline.com

Insight into the Structural Evolution of Porous and Fractured Media by Forced Aeration during Heap Leaching

Niranjan Behera[1], Prajna Kar[2], Priyabrata Jena[3]

[1]Department of Mechanical Engineering, Raajdhani Engineering College, Bhubaneswar, Odisha
[2]Department of Mechanical Engineering, NM Institute of Engineering and Technology, Bhubaneswar, Odisha
[3]Department of Mechanical Engineering Capital Engineering College, Bhubaneswar, Odisha

A b s t r a c t

Despite lots of techniques in improving the heap leaching performance, many constraints on the indus- trial applications remain. We proposed a correspondingly effective and new idea of introducing forced aeration to improve the bad permeability and leaching effect of Yangla Copper Mine (YCM) during heap leaching. The dual-media theory was employed to study the impact mechanism of forced aeration on the variations of porous and fractured media during the column leaching experiments. An X-Ray Computed Tomography (CT) set was utilized to perform the pore imaging of the specimens and the fracture morphology of the particles within the columns was analyzed by Scanning Electron Microscope (SEM) as aeration rate (AR) changed. The results show that there exists copious fine particles within the heap of YCM, the particle size distribution of which is not reasonable. The forced aeration can not only promote the development of the porous and fractured structures but effectively break the blocked seepage paths. Then the leaching degree is improved and the seepage performance of the solute within the solution is enhanced. Therefore, the forced aeration is probable of making the leaching performance greatly improved.

1. Introduction

Heap leaching is a hydrometallurgical extraction technique commonly utilized in recovering valuable metals from refractory or low-grade ores [1]. With operational simplicity, relatively low costs, high recovery rates, short construction time and environmental advantages, this method has become more and more prevalent in the mineral processing industries [2]. The leaching system is constituted by solid-liquid-gas phases, the interaction degree of which depends on the permeability coefficient of the system. Hence, the leaching effect is strongly influenced by the permeability of the system. However, due to the mechanical compaction and weathering, permeability of the ore dump is usually poor.

The research community has proposed many methods to increase the leaching performance by loosening the dump, introducing external electric field, presenting stress wave, adding catalysts and accelerating the growth of microorganisms, etc. [3]. Currently, aeration assisted heap leaching has become a relatively new and effective leaching technique employed in improving leaching efficiency. Despite lots of studies on the influence of aeration in increasing the leaching rate, the experts and scholars worldwide mainly stressed the role of aeration played in oxygen or carbon dioxide supply and few of which studied the influence of aeration on permeability of the heap. Brierley et al. held that whether aeration should be employed in heap leaching had become the core issue limiting the development of leaching mining [4]. Therefore, it is of great significance to exactly understand the enhanced leaching mechanism by forced aeration.

The leaching dump is a media constituted of irregular ore particles with bulks of pores and fractures. We have shown in a previous study that aeration can effectively improve the leaching effect based on MRI characterization, however, it did not involve the impact on fractures within the ore particles. Hence, during heap leaching, a concept of porous and fractured media was utilized to study the influence of aeration [5]. In this concept, two kinds of seepage channels, i.e., pore and fracture, were thought to be naturally present within the heap [6]. On one hand, the pore structure was the dominant channel for solution flow. On the other hand, fractures in ore particles were the second liquid flowing channels. Despite the relatively poor penetrability, the numerous fractures could still provide adequate storage space for the solution. Hence, a favorable environment for leaching would be obtained under the coupling effect of porous and fractured media [7,8].

Table 1
Particle size distribution of the ore.

Size (mm)	Cumulative weight (%, by weight)	Size (mm)	Cumulative weight (%, by weight)
0.125	0.34	4.000	70.65
0.300	1.51	5.000	87.41
0.450	3.79	6.000	91.04
1.000	7.56	7.000	95.35
2.000	30.23	8.000	97.35
3.000	50.89	9.000	100.00

In order to clearly understand the influence of aeration rate (AR) on leaching performance, this study investigates two factors: the influence of air pumped into the novel leaching columns on the pore changes using X-ray computed tomography (CT) and the evolution of fractures within ore particles using scanning electron microscope (SEM).

2. Experimental

Ore

About 3000 g samples were obtained from the leaching dump of Yangla Copper Mine (YCM) located in Yunnan province of China, particle size distribution of which was detailed in Table 1.

Fig. 1 depicts the particle size distribution curve of the samples, the type of which belonged to A according to the particle size distribution curves customary in the geotechnical engineering area [9]. So, it could be speculated that there are bulk of loose particles within the leaching dump of YCM which made the heap highly compacted.

The main chemical components of the samples are shown in Fig. 2.

Analytically, the average particle size of the samples was relatively small [10]. And the alkaline components such as MgO, CaO, Fe_2O_3 and Al_2O_3, the content of which was more than 40%, might lead to a high acid consumption rate during heap leaching. Thus, improving permeability of the dump using some techniques, such as aeration, could be better ways of increasing the leaching efficiency for YCM [11,12].

Column leaching experiment

Experimental setup and leaching solution

A novel heap leaching apparatus schematically presented in Fig. 3 is utilized to conduct the column leaching experiments as AR changed. This apparatus was mainly consisted by the leaching columns (fabricated by plexiglass), solid-liquid-gas circulation system, control cabinet and computer, the maximum AR of which allowed for the experiments was 0.5 m^3/h.

As noted in Fig. 3, R1, R1 and R3 are raised barrels; S1, S1 and S3 are specimens; T1, T2 and T3 are collecting barrels; U1, U2 and U3 are inflating inlets; V1, V2 and V3 are perforated plates; and W1, W1 and W3 are sealing layers.

The pore imaging was performed on a spiral CT set (SOMATOM Sensation 16), and SEM (JEOL JSM-6701F) was employed to analyze fracture morphology of the particles. Then, the sulphuric acid (pH = 1) purchased from a firm in Beijing was utilized alone, in order to avoid the effects of other chemical reagents, to be leaching solution for the experiments [13–15].

Preparation

As shown in Fig. 3, the samples were well mixed according to Table 1, evenly (700g) packed into the three columns and named S1, S2 and S3. Then, three equally-sized pebbles (the three black

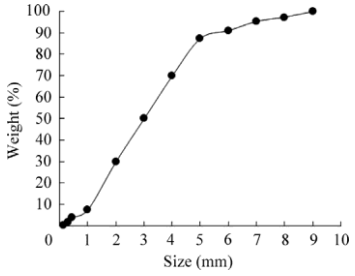

Fig. 1. Particle size distribution curve of the samples.

Fig. 2. Main chemical composition of the samples.

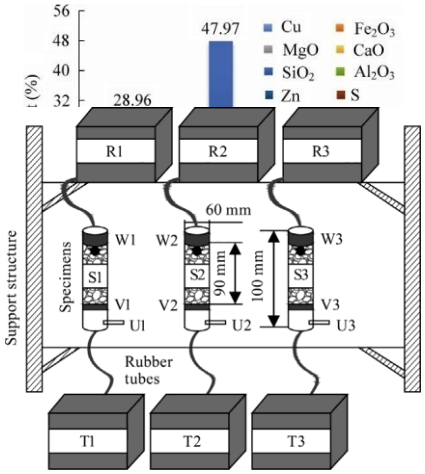

Fig. 3. Schematic of the novel column leaching apparatus.

spots in Fig. 3) with a diameter of 2.5 mm were laid on top of the particles within the three specimens and named A, B and C. During liquid circulation, the three specimens would be saturated for 24 h.

Operation

(1) Before air was pumped into the specimens, CT and SEM were separately utilized to perform the original imaging of the pore structures of S1, S2 and S3 and the fracture morpholo-
gies of A, B and C. During CT imaging, the magnification and minimum resolution cell were 4.14 and 46.9 lm respec- tively, and layer number of the specimens was 1500 with a thickness of 4 lm. It used a projected amplitude of 400, a rotation step of 0.9°, a tube voltage of 120 kV and a tube
current of 160 lA respectively. This moment was defined to be 0 d.

(2) Air was pumped into S1, S2 and S3, ARs of which were 0, 0.3 and 0.5 m^3/h respectively. Then CT and SEM were repeatedly employed to perform the images as leaching time changed (10, 20, 30 and 40 d).

(3) CT images were thresholded in Matlab to conduct the 3D reconstructions to analyze pores changes, model sizes of which were all 25.8 mm × 25.8 mm in the x and y directions

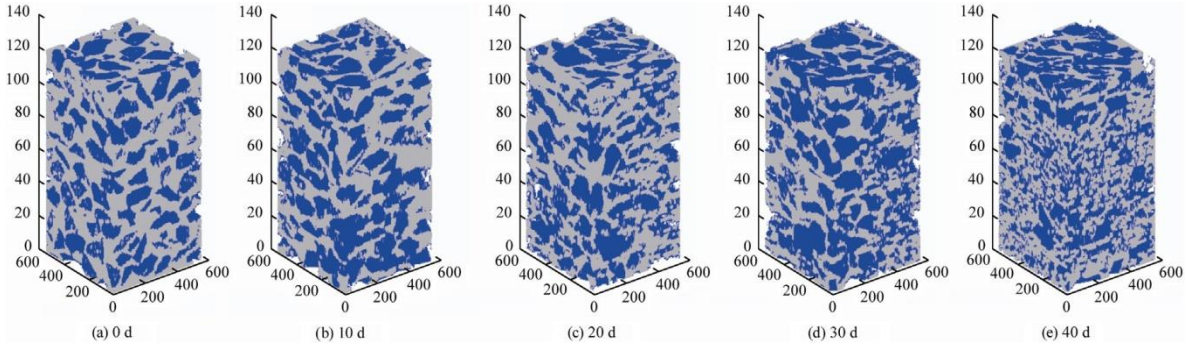

Fig. 5. 3D models of S2 as time changes.

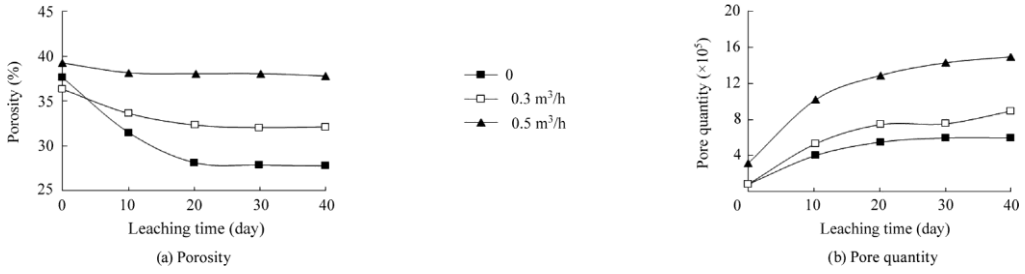

Fig. 6. Pore changes as ARs and time change.

and 80.0 mm in the *z* direction [16]. SEM images were imported in Image J and Fractal Fox to study the evolution of fractures.

3. Results and discussion

Pore changes

The 2D CT images and the corresponding binary images acquired from S1, S2 and S3 as AR changes are presented in Fig. 4 (e.g., 10 d), the sizes of which were all 850 pixel× 850 pixel in the *x* and *y* directions. Obvious differences occurred in the distribution of particles and pore structures. Particle sizes in S2 (Fig. 4b and e) and S3 (Fig. 4c and f) were smaller than that in S1 (Fig. 4a and d).

Taking S2 as an example, Fig. 5 shows the 3D reconstruction models of pore structures as leaching time changed, of which, the blue and grey represented the leaching solution and ore particles respectively. It could be seen that as time developed, sizes of the ore particles within the specimens got smaller, the number of which was increased to make the porous structure hard-packed.

The porosity of the specimens could be expressed as Eq. (1) [17].

$$n = \left(1 - \frac{V_a}{V}\right) \times 100\% \quad (1)$$

where n, V_a and V are the porosity, solid volume and whole volume of the models, respectively.

Within S1, S2 and S3, the porosity and pore quantity as time changes are calculated and shown in Fig. 6.

Fig. 6a shows that as AR and time change, the porosity of S1 reduces from approximately 38% to 31.8% after 10 d. However, they are relatively slow in S2 and S3. Using S3 as an example, the decline rate of porosity is only about 2%. Analytically, aeration would be substantially advantageous to the solute transport within the leaching solution, and this made the seepage paths less likely to be blocked. Therefore, porosity of the aerated system could be kept at a comparatively high level. Fig. 6b shows that the number of pores within all the three specimens all increases, however in S1, it is relatively slow, and indicates that aeration might not only shorten the leaching time but improve the reaction degree to push forward the development of the pore structure.

Evolution of fractures

As shown in Fig. 7 (e.g., 20 d), SEM images of A, B and C are acquired, then based on a specified threshold, the binary images are obtained [18,19]. There exists a small amount of fine fractures on the surface of A. However, many open fractures occurred in B and C, and fractures in the latter were wider and deeper. It indicated that aeration might increase the leaching degree by expand-

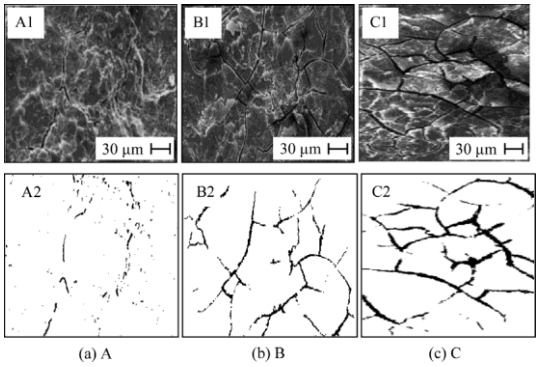

Fig. 7. SEM and its binary images of specimens (20 d).

ing the fractured structure of particles. Moreover, a higher AR was more beneficial.

In this work, the fractal geometry theory was utilized to analyze the complicated fracture morphologies of A, B and C [20,21]. The fractal dimension, in calculation, usually referred to fractal box dimension (FBD). In this work, $F \subset R^n$ was assumed to be an arbitrary set that was non empty and bounded, and $N_\delta(F)$ represented the minimal number of the sets, the maximum diameter of which was δ in covering F set. Then, the upper and lower FBDs of F set could be calculated according to equation [22].

$$\begin{cases} \underline{\dim}_B F = \lim\limits_{\delta \to 0} \inf \dfrac{\lg N_\delta(F)}{-\lg \delta} \\ \overline{\dim}_B F = \lim\limits_{\delta \to 0} \sup \dfrac{\lg N_\delta(F)}{-\lg \delta} \end{cases} \quad (2)$$

If $\underline{\dim}_B F$ is equal to $\overline{\dim}_B F$, FBD of F set can now be expressed by

$$\dim_B F = \lim_{\delta \to 0} \frac{\lg N_\delta(F)}{-\lg \delta} \quad (3)$$

In order to clearly understand the effect of aeration on the evolution of fractures during heap leaching, FBDs of A and C as time changed were calculated. The two linear correlation coefficients R1 and R2 were 0.9256 and 0.9322 respectively, indicating that the models were effective. Based upon the binary images and results of FBDs of A and C, the evolution curves of fractures as leaching time developed were calculated, analyzed by Origin and depicted in Fig. 8. FBD of C is always higher than that of A, as shown in Fig. 8a, indicating that the amount of fractures within C is more than that in A. From Fig. 8b, it could be drawn that the fracture width of C was bigger than that of A, illustrating that aeration could effectively widen the fractures within the particles to accommodate more leaching solution, and this might improve the leaching efficiency [23].

During heap leaching, the development of fractures was a dynamic changing process which could result in a variable permeability coefficient. Thence, the seepage state within the heap was probable of being influenced. The capillary buddle model was employed to study the dynamic-permeability coefficient (DPC) and fracture ratio (DFR) of A and C, calculated by [24–27].

$$\begin{cases} e = \dfrac{k_{1a}^3}{12 g^o} \dfrac{y_x}{[2(u_1 - y_x)]} \left(1 - k^{-2(u_1 - y_x)}\right) \\ b = \dfrac{k_{1a}}{g^o y_x (u_1 - 2/k^{y_x (u_1 - 2)})} - 1 \end{cases} \quad (4)$$

where e and b are DPC and DFR respectively; k_{1a} and k_{2a} the maximum fracture width and capillary diameter respectively; y_x the fitting equation between FBD and time; $/ = L_c/L_m$ the fracture tortuosity; L_c and L_m the average length of the channels and length of the object area; and g^o the unit depth of the fractures.

Taking particle A as an example ($y_1 = 1.9054 + 0.0835x$), DPC (e_A) and DFR (b_A) calculation model of A could be calculated as

$$1.19054 + 0.00835 \cdot x$$

$$\begin{cases} e_A = \dfrac{k_{1a}^3}{12 g^o} [2(u_1 - 1.19054 - 0.00835 \cdot x)] \\ b_A = k_{1a} \dfrac{(1.19054 + 0.00835 \cdot x)(u_1 - 2/k)}{g^o (1.19054 + 0.00835 \cdot x)(u_1 - 2)} \times \left(1 - \dfrac{1}{k^{1.19054 + 0.00835 \cdot x - 2}}\right) \end{cases} \quad (5)$$

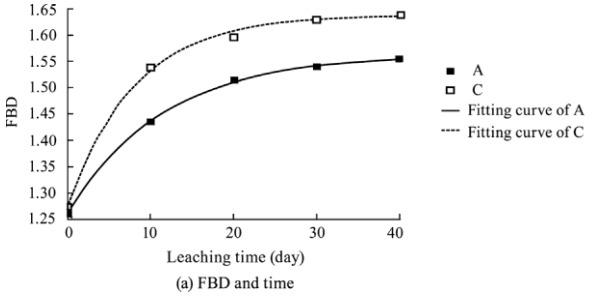

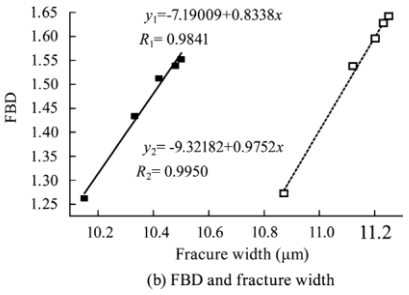

Fig. 8. The evolution curves of FBD & time and FBD & fracture width.

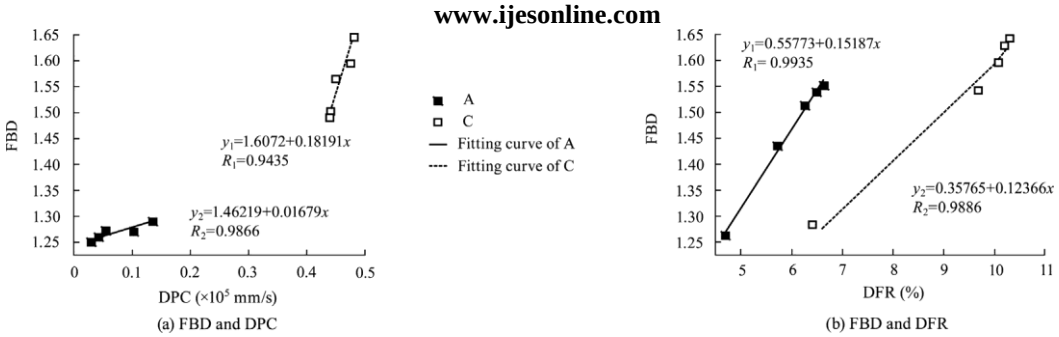

Fig. 9. The evolution curves of FBD & DPC and FBD & DFR.

Then, according to the calculation models of A and C, DPC and DFR of which are depicted in Fig. 9. From Fig. 9a, it could be seen that the average DPC of C (0.46×10^{-5} mm/s) was obviously higher than that of A (0.09×10^{-5} mm/s). Fig. 9b shows the average DFR of C (10.2%) is higher than that of A (6.3%). It indicates that during heap leaching, the forced aeration could promote the development of fractures within ore particles. This would be beneficial in improving the permeability coefficient of the whole system to provide tremendous convenience for the solution flow.

4. Conclusions

The column leaching experiments were conducted to study the impact of different aeration rates (ARs) on the changes of porous and fractured media using X-ray CT and SEM. The analysis results of the samples obtained from the ore heap of Yangla copper mine indicated a bad particle distribution. Experimental results from a CT set showed that pore structure within the three specimens (S1, S2 and S3), when AR was different, changed differently. When AR increased, the porosity of S2 (0.3 m^3/h) and S3 (0.5 m^3/h) became higher than that of S1 (without aeration), and particles in S2 and S3 were more loose and fine than that in S1. Experiments analyzed by SEM showed that the fractal box dimensions, dynamic porous and fractured performance of particles B (0.3 m^3/h) and C (0.5 m^3/h) were all better than that of A (without aeration).

The forced aeration, especially in abiotic heap leaching, could not only promote the development of pore structure between the particles but accelerate cracking rate of the fractures within the particles. Accordingly, the contact area of solution and particles increased, and this brought a higher leaching rate and reaction degree. Thence, the leaching efficiency and performance of the ore were probable of being significantly improved.

Acknowledgments

The authors would like to acknowledge and thank the National Natural Science Foundation of China (No. 51374035), the Foundation for the Author of National Excellent Doctoral Dissertation of PR China (No. 201351) and the Program for New Century Excellent Talents in University of China (No. NCET-13-0669).

References

[1] Cariaga E, Concha F, Sepúlveda M. Flow through porous media with applications to heap leaching of copper ores. Chem Eng J 2005;111(2):151–65.
[2] Laman JT. Solution mining and in-situ leaching. Mining environmental handbook: effects of mining on the environment and american environmental controls on mining; 2014.
[3] Brierley JA, Brierley CL. Present and future commercial applications of biohydrometallurgy. Hydrometallurgy 1999;9(2–3):81–9.
[4] Winterfeld PH, Wu YS. Simulation of coupled thermal-hydrological-mechanical phenomena in porous and fractured media. Spe Journal 2015;12 (1):369–83.
[5] Song JW, Wang MY, Tang DW. Experiment on water infiltration and solute migration in porous and fractured media. Adv Mater Res 2014:955–959:1993–7.
[6] Zhang Y, Yao F, Xu D, Ma B, Yao H. Stochastic simulation on preferential seepage channels in water-flooding reservoirs. Electron J Geotech Eng 2015;20 (2):803–12.
[7] Nikolaevskij VN. Mechanics of porous and fractured media. World Scientific; 1990.
[8] Tartakovsky AM, Meakin P, Scheibe TD, Wood BD. A smoothed particle hydrodynamics model for reactive transport and mineral precipitation in porous and fractured porous media. Water Resour Res 2007;43(5):5437.
[9] Ai CM. Experimental and theory study on strengthening leaching of copper ores by surfactant. Beijing: University of Science and Technology Beijing; 2015.
[10] Wu AX, Zhang J, Jiang HC. Improvement of porosity of low-permeability ore in heap leaching. Min Metall Eng 2006;26(6):5–8.
[11] Thansandote P, Harris RM, Dexter HL, Simpson Graham L, Pal Sandeep, Upton Richard J, Valko Klara. Improving the passive permeability of macrocyclic peptides: balancing permeability with other physicochemical properties. Bioorg Med Chem 2015;23(2):322–7.
[12] Zuo H, Wang YM, Chen XS, Jiang HC. Mechanism of improving permeability in dump by effect of electric field. Chin J Nonferr Metals 2007;17(3):471–5.
[13] Lizama HM. Copper bioleaching behavior in an aerated heap. Int J Miner Process 2001;62(1–4):257–69.
[14] Paul M, Di WR. An improved method for heap leaching of chalcopyrite. Patent: WO 2000071763 A1; 2000.
[15] Mohammadreza Fatahi, Mohammad Noaparast, Ziaeddin Shafaei Seyyed. Nickel extraction from low grade laterite by agitation leaching at atmospheric pressure. Int J Min Sci Technol 2014;24(4):543–8.
[16] Gardner RJ, Kiderlen M. A new algorithm for 3D reconstruction from support functions. IEEE Trans Pattern Anal Mach Intell 2009;31(3):556–62.
[17] Rehder B, Banh K, Neithalath N. Fracture behavior of pervious concretes: The effects of pore structure and fibers. Eng Fract Mech 2014;118(2):1–16.
[18] Li Y, Zeng LJ. Analyzing the grating profile parameters based on scanning-electron microscope images. Key Eng Mater 2008;381–382:299–300.
[19] Hs H, Chabaat M, Thimus JF. Use of scanning electron microscope and the non-local isotropic damage model to investigate fracture process zone in notched concrete beams. Exp Mech 2007;47(4):473–84.
[20] Zhou Z, Su Y, Wang W, Yan Y. Application of the fractal geometry theory on fracture network simulation. J Pet Explor Prod Technol 2016:1–10.
[21] Sheng JL, Wu YL. Study on the distribution characteristics of the structural planes in rock mass based on the fractal geometry theory. Metal Mine 2002;11 (2):231–5.
[22] Ai T, Zhang R, Zhou HW, Pei JL. Box-counting methods to directly estimate the fractal dimension of a rock surface. Appl Surf Sci 2014;314(10):610–21.
[23] Lagno Sanchez FA, Acuña GMG. Process for recovery of technical grade molybdenum from diluted leaching acid solutions (PLS), with highly concentrated arsenic, from metallurgical residues. US patent: US9279168; 2016.
[24] Ju XD, Feng WJ, Zhang YJ, Zou ZS. A capillary bundle model based on aperture's exponential distribution and its application in porous media's mono direct percolation. Adv Mater Res 2012;594–597:2481–5.
[25] Xu J, Wang Z, Ren J, Yuan J. Experimental research on permeability of undisturbed loess during the freeze-thaw process. J Hydraul Eng 2016;47 (9):1208–17.
[26] Ghashghaei HT, Hassani A. Investigating the relationship between porosity and permeability coefficient for pervious concrete pavement by statistical modelling. Mater Sci Appl 2016;07(2):101–7.
[27] Yu BY, Chen ZQ, Ding QL, Wang LZ. Non-Darcy flow seepage characteristics of saturated broken rocks under compression with lateral constraint. Int J Min Sci Technol 2016;26(6):1145–51.